The Effects of Migration and Connectivity upon Initial Behavior of Multi-City Endemic Models

MTBI-02-05M

Alan Covert [1], Laiza Espinoza [2], Matthew Hoffman [3]

[1] Department of Mathematics and Statistics, Arizona State University, Tempe, AZ

[2] Department of Bioengineering, Arizona State University West, Phoenix, AZ,

[3] Department of Mathematics, New Mexico Institute of Mining and Technology, Socorro, NM

Abstract

We consider the behavior of an infectious disease over a system of networked cities with SLIR dynamics. Two models are studied: one with a partition between traveler and resident populations, and another without. R_0 is computed for both the partitioned and non-partitioned models. Numerical solutions of the nonlinear dynamical systems are performed in order to gain insight into the initial behavior and intercity spread of disease, and system response to dispersal volumes and number of connections between cities is also studied. We consider a theoretical future disease with SARS-like parameters, and run numerical solutions using parameters from past studies on SARS.

1 Introduction

Modern developments in mass transit have created contact points between geographical regions that beforehand could not interact on a timescale of biological importance. Diseases that once could have been isolated in a specific region of the world now have the ability to jump from one location to another in a matter of hours, and may have the opportunity to develop an epidemic if the new location is sufficiently conducive to disease growth. Recently the outbreak of SARS in China has presented such a problem. Even after the local epidemic was contained a small number of travelling infected individuals expanded the infection to provinces in Canada.

Similarly, if a previously unknown highly infectious disease were to be introduced into the air traffic of the United States, it would be beneficial to understand how migration rates affect the ability of the disease to establish itself independently in new cities. The mathematical model presented here is used to determine the impact of travel on the spread of a moderately infectious disease. We work with a general model for a system with n cities, looking only at short time intervals (the beginning phase of an epidemic) where the disease can be introduced to new cities by air travel.

2 Background

Modeling the spread of a disease over city networks has been increasingly important over the past few decades. An early discrete-time multi-city model was presented by Rvachev and Longinie [14] in 1985. More recent work has been presented by Hyman and LaForce [12], Arino and van den Driessche [1], [2], [3], [9], Castillo-Chavez, Song, et al. [4], Chowell and Castillo-Chavez [5], [6] and others.

A similar model to the ones presented here was presented by Hyman and LaForce [12], in which they modify an SIRP (Susceptible, Infected, Recovered, Protected) model to look at the spread of Influenza within a network of cities. The susceptible and infected populations mix randomly within each city. The SIRP transmission model is extended to predict the spread of the virus among multiple cities, with the assumption that infection does not occur during the actual act of transit. Travel is modelled as a constant flow between cities, and it is assumed that everyone in each city has an opportunity to travel.

Castillo-Chavez, Song et al. [4] present an SLIR model for the spread of disease within New York, distinguishing between people who use the subway system and those who do not. In any particular neighborhood of the city, non-subway users (NSU) interact with people in their own neighborhood (both with other non-subway users and with subway users), while subway users also interact with people from other neighborhoods due to their contact interaction on the subway system.

In researching methods for analysis of our model we also consider work done by Arino et al.[1] on the spread of an epidemic within a system of multiple spatial patches and multiple species. They develop an SEIR model and use a mobility matrices similar to the models presented here. Our model can be analyzed using methods adapted from those presented in their work.

3 Partitioned SLIR Model

We present a general model for an n-city system, looking primarily at short time intervals (the beginning phase of an epidemic) where the disease is introduced to new cities by air travel. We use two partitions consisting of a Traveler population and a Resident population to better model the fact that not everyone in a city is likely to travel frequently during the timescale of an epidemic. The Traveler partition is assumed to be a constant proportion of the total population, and the Resident partition is composed of the remainder. We use the term migration interchangeably with daily intercity travel.

Each partition has four classes (Susceptible, Latent, Infected, and Recovered). For any city i, the total outgoing migrations for any class can be described as the summation of migrations to that same class in all other cities j, where j takes integer values from 1 to n. These migrations can be written as α_{ji} (where α_{ji} is the migration, in people per day, from the Traveler partition of city i to that of city j) multiplied by the proportion of that class in the total traveler population; for example, the migration of susceptibles from city

i to city j would be written as $\alpha_{ji}\frac{S_{Ti}}{N_{Ti}}$. Similarly, the inward migrations of susceptibles from city j to city i would be written as $\alpha_{ij}\frac{S_{Tj}}{N_{Tj}}$.

For both the Traveler and Resident partitions within city i, susceptible individuals can become infected at a rate proportional to their possible contacts with infected individuals from either compartment; for example, susceptible travelers become infected at rate $\frac{\beta S_{Ti}(I_{Ti}+I_{Ri})}{N_i}$. They then have a latent infection, and can progress from latency to infectiousness at a rate kL_{Ti}. Finally, they can recover at the rate γI_{Ti}.

Because we are only interested in brief early stages of an epidemic, we assume that there is no time for re-infection of recovered individuals. Behavioral effects and a disease-induced death rate, although probably quite significant for longer time periods, are also omitted in our analysis. Natural birth and death rates are included for demographic renewal.

See Figure 1 for the state diagram. From this figure we derive a system of nonlinear ODE's with parameters described in Table 1.

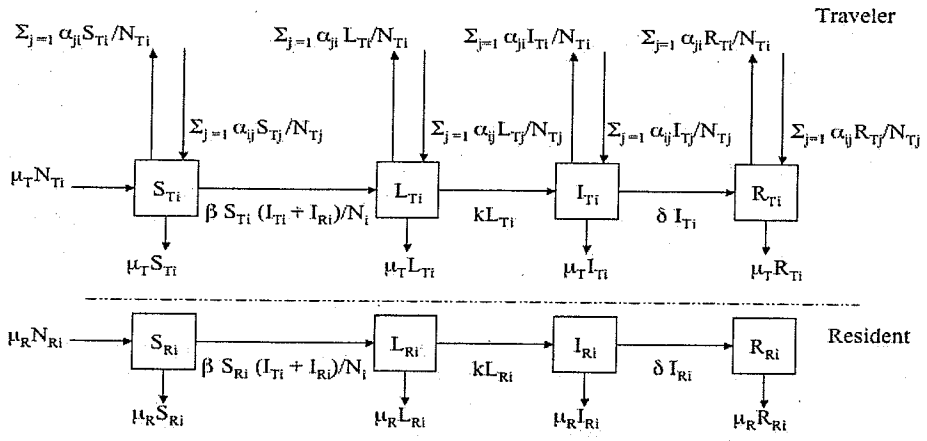

Figure 1: State Diagram for Partitioned Model

Parameter/State	Meaning	Units
μ_R	Residents Birth/Death Rate	day^{-1}
μ_T	Traveler Birth/Death Rate	day^{-1}
μ	Birth/Death Rate	day^{-1}
α_{ij}	Rate of travel from city j to city i	$persons(day^{-1})$
β	Rate of Infection	day^{-1}
k	Rate of Incubation	day^{-1}
γ	Rate of Recovery	day^{-1}
S_{Ti}	Susceptible Travelers at city i	$persons$
L_{Ti}	Latent Travelers at city i	$persons$
I_{Ti}	Infected Travelers at city i	$persons$
R_{Ti}	Recovered Travelers at city i	$persons$
S_{Ri}	Susceptible Residents at city i	$persons$
L_{Ri}	Latent Residents at city i	$persons$
I_{Ri}	Infected Residents at city i	$persons$
R_{Ri}	Recovered Residents at city i	$persons$
N_i	Total population of city i	$persons$
N_{Ri}	Total population of Residents of city i	$persons$
N_{Ti}	Total population of Travelers of city i	$persons$

Table 1: Model Parameters and States

3.1 Model Equations for Partitioned n-City System

$$S'_{Ti} = \mu_T N_{Ti} - \mu_T S_{Ti} + \sum_{j=1}^{n} \alpha_{ij} \frac{S_{Tj}}{N_{Tj}} - \sum_{j=1}^{n} \alpha_{ji} \frac{S_{Ti}}{N_{Ti}} - \frac{\beta S_{Ti}(I_{Ti} + I_{Ri})}{N_i}$$

$$L'_{Ti} = \frac{\beta S_{Ti}(I_{Ti} + I_{Ri})}{N_i} - \mu_T L_{Ti} + \sum_{j=1}^{n} \alpha_{ij} \frac{L_{Tj}}{N_{Tj}} - \sum_{j=1}^{n} \alpha_{ji} \frac{L_{Ti}}{N_{Ti}} - kL_{Ti}$$

$$I'_{Ti} = kL_{Ti} - \mu_T I_{Ti} + \sum_{j=1}^{n} \alpha_{ij} \frac{I_{Tj}}{N_{Tj}} - \sum_{j=1}^{n} \alpha_{ji} \frac{I_{Ti}}{N_{Ti}} - \gamma I_{Ti}$$

$$R'_{Ti} = \gamma I_{Ti} - \mu_T R_{Ti} + \sum_{j=1}^{n} \alpha_{ij} \frac{R_{Tj}}{N_{Tj}} - \sum_{j=1}^{n} \alpha_{ji} \frac{R_{Ti}}{N_{Ti}}$$

$$S'_{Ri} = \mu_R N_{Ri} - \mu_R S_{Ri} - \frac{\beta S_{Ri}(I_{Ti} + I_{Ri})}{N_i}$$

$$L'_{Ri} = \frac{\beta S_{Ri}(I_{Ti} + I_{Ri})}{N_i} - kL_{Ri} - \mu_R L_{Ri}$$

$$I'_{Ri} = kL_{Ri} - \gamma I_{Ri} - \mu_R I_{Ri}$$

$$R'_{Ri} = \gamma I_{Ri} - \mu_R R_{Ri}$$

4 Non-Partitioned SLIR Model

From the Partitioned Model we derived a simplified model for the spread of a disease within a network of cities (Figure 2). This model assumes that everyone has the opportunity to travel, and thus the Resident partition is omitted. This model also includes birth and death rates, while a disease induced death rate is omitted. The migration (travel) rate is represented by α_{ij}, which is read as the migration from city j to city i. These migrations are also multiplied by by the proportion of that class in the total traveler population; for example, the migration of susceptibles from city i to city j would be written as $\alpha_{ji}\frac{S_{Ti}}{N_{Ti}}$. Due to the nature of the equations the system's total population is maintained constant, and for balanced migration, the population of any given city is constant as well. It is assumed that recovered individuals cannot be reinfected, since the model is intended for a short time interval at the beginning of an epidemic.

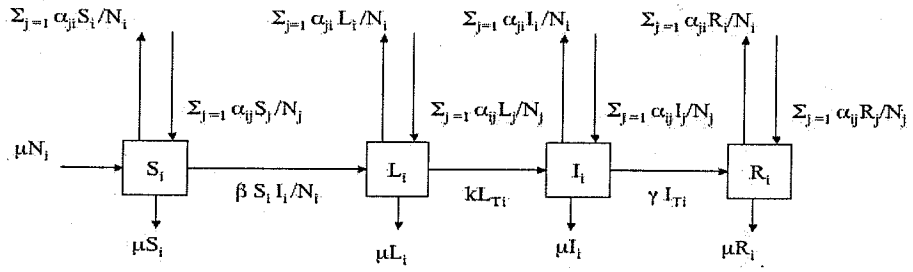

Figure 2: State Diagram for Non-Partitioned Model

4.1 Model Equations for Non-Partitioned System

$$S_i' = \mu N_i - \mu S_i + \sum_{j=1}^{n} \alpha_{ij}\frac{S_j}{N_j} - \sum_{j=1}^{n} \alpha_{ji}\frac{S_i}{N_i} - \beta S_i \frac{I_i}{N_i}$$

$$L_i' = \beta S_i \frac{I_i}{N_i} - \mu L_i + \sum_{j=1}^{n} \alpha_{ij}\frac{L_j}{N_j} - \sum_{j=1}^{n} \alpha_{ji}\frac{L_i}{N_i} - kL_i$$

$$I_i' = kL_i - \mu I_i + \sum_{j=1}^{n} \alpha_{ij}\frac{I_j}{N_j} - \sum_{j=1}^{n} \alpha_{ji}\frac{I_i}{N_i} - \gamma I_i$$

$$R_i' = \gamma I_i - \mu R_i + \sum_{j=1}^{n} \alpha_{ij}\frac{R_j}{N_j} - \sum_{j=1}^{n} \alpha_{ji}\frac{R_i}{N_i}$$

5 Analysis

For our system we need to know how R_0 depends on migration in order to determine whether the persistence of the disease in a city is dependent on the migration. We find that even though the R_0 is dependent of the migrations, with the values of populations and migrations from the 34 largest cities in the United States, the proportional migration terms are significantly smaller then the infection and recovery rate. Taking the migration terms to approach zero we found that R_0 becomes the same as a single SLIR model.

6 The Basic Reproductive Ratio R_0

In calculating R_0 for this system the method demonstrated by Julian Arino and Pauline van den Driessche [3] was used. In their work they use the next generation operator given

by Diekmann and Heesterbeek [8] but due to the symmetry of the system of equations they are able to reduce the dimensions of the matrices used in the process. They separate both the F and V matrices into four block matrices apiece. For the non-partitioned model with $4n$ equations for n cities this method reduces a $2n \times 2n$ matrix to an $n \times n$ matrix. For the partitioned model with $8n$ equations it is reduces a $4n \times 4n$ matrix to a $2n \times 2n$ matrix.

6.1 R_0 for a Non-Partitioned Model with n Cities

To begin make the substitutions $m_{ij} = \frac{\alpha_{ij}}{N_j}$ to simplify the expressions.Next the disease free equilibrium must be found. The disease free equilibrium, denoted often as DFE, is the values of which the populations of each class approaches in the absence of a disease. Letting $\sum_{j=1}^{n} I_i = 0$ and $\sum_{j=1}^{n} L_i = 0$. Then as time continues the value of $\sum_{j=1}^{n} R_i$ approaches zero as time continues since its population is being reduced by death and it is not being replenished by the infected class. Since the population is constant for the system $\sum_{j=1}^{n} S_i = \sum_{j=1}^{n} N_i$. Also since the population of each city is constant $S_i = N_i$ at the DFE.

To generate the F and V matrices first define a vector $X = (L_1, L_2, \ldots, L_n, I_1, I_2, \ldots, I_n)^T$ then separate the terms of the infected and latent equations that represent new infections from the remaining terms. The new infections are then written as a new vector, denoted here as f while the negative of the remaining terms are represented in another vector, v

$$f = \begin{pmatrix} \beta\frac{S_1 I_1}{N_1} \\ \beta\frac{S_2 I_2}{N_2} \\ \vdots \\ \beta\frac{S_n I_n}{N_n} \\ 0 \\ \vdots \\ 0 \end{pmatrix}, v = \begin{pmatrix} (\mu+k)L_1 - \sum_{j=1}^{n} m_{1j}L_j + \sum_{j=1}^{n} m_{j1}L_1 \\ (\mu+k)L_2 - \sum_{j=1}^{n} m_{2j}L_j + \sum_{j=1}^{n} m_{j2}L_2 \\ \vdots \\ (\mu+k)L_n - \sum_{j=1}^{n} m_{nj}L_j + \sum_{j=1}^{n} m_{jn}L_n \\ (\mu+k)I_1 - \sum_{j=1}^{n} m_{1j}I_j + \sum_{j=1}^{n} m_{j1}I_1 - kL_1 \\ (\mu+k)I_2 - \sum_{j=1}^{n} m_{2j}I_j + \sum_{j=1}^{n} m_{j2}I_2 - kL_2 \\ \vdots \\ (\mu+k)I_n - \sum_{j=1}^{n} m_{nj}I_j + \sum_{j=1}^{n} m_{jn}I_n - kL_n \end{pmatrix}$$

Now let $F = \frac{\delta f}{\delta X}$ and $V = \frac{\delta v}{\delta X}$. The F and V matrices here will be $2n \times 2n$ and can then be divided into a total of eight block matrices such that

$$F = \begin{pmatrix} 0 & G \\ 0 & 0 \end{pmatrix}, V = \begin{pmatrix} A & 0 \\ C & B \end{pmatrix}$$

where G,A,B and C are $n \times n$ matrices

Evaluating the F and V matrices with $S_i = N_i$ and $R_i = 0$ from the DFE the matrices G,A,B and C will be of the form

$$A = \begin{pmatrix} \mu + k + \sum_{j=1}^{n} m_{j1} & -m_{12} & \cdots & -m_{1n} \\ -m_{21} & \mu + k + \sum_{j=1}^{n} m_{j2} & \cdots & -m_{2n} \\ \vdots & & \ddots & \vdots \\ -m_{n1} & -m_{n2} & \cdots & \mu + k + \sum_{j=1}^{n} m_{jn} \end{pmatrix}$$

$$B = \begin{pmatrix} \mu + \gamma + \sum_{j=1}^{n} m_{j1} & -m_{12} & \cdots & -m_{1n} \\ -m_{21} & \mu + \gamma + \sum_{j=1}^{n} m_{j2} & \cdots & -m_{2n} \\ \vdots & & \ddots & \vdots \\ -m_{n1} & -m_{n2} & \cdots & \mu + \gamma + \sum_{j=1}^{n} m_{jn} \end{pmatrix}$$

$$G = \begin{pmatrix} \beta & 0 & \cdots & 0 \\ 0 & \beta & & 0 \\ \vdots & & \ddots & \vdots \\ 0 & 0 & \cdots & \beta \end{pmatrix}, C = diag(-k)$$

Applying the property demonstrated by Arino and van den Driessche an inverse of matrix V can be found from the block matrix form. Then R_0 will be the spectral radius or dominant eigenvalue of the FV^{-1} matrix.

$$V^{-1} = \begin{pmatrix} A^{-1} & 0 \\ B^{-1}CA^{-1} & B^{-1} \end{pmatrix}$$

$$FV^{-1} = \begin{pmatrix} 0 & G \\ 0 & 0 \end{pmatrix} \begin{pmatrix} A^{-1} & 0 \\ B^{-1}CA^{-1} & B^{-1} \end{pmatrix} = \begin{pmatrix} GB^{-1}CA^{-1} & GB^{-1} \\ 0 & 0 \end{pmatrix}$$

Since the lower row of FV^{-1} consists of zero matrices any non zero eigenvalues of FV^{-1} are also eigenvalues of $GB^{-1}CA^{-1}$. Thus Arino and van den Driessche conclude that R_0 is the spectral radius of the matrix $GB^{-1}CA^{-1}$; that is,

$$R_0 = \rho(GB^{-1}CA^{-1})$$

, where $\rho(X)$ is defined to be the spectral radius of a matrix X.

6.2 R_0 for a Non-Partitioned Model with 2 Cities

The smallest non-partitioned model of interest is that with two cities. For the matrices A and B, we have

$$A = \begin{pmatrix} \mu + \gamma + m_{21} & -m_{12} \\ -m_{21} & \mu + \gamma + m_{12} \end{pmatrix},$$

$$B = \begin{pmatrix} \mu + k + m_{21} & -m_{12} \\ -m_{21} & \mu + k + m_{21} \end{pmatrix}.$$

Taking the inverse of A and B yields:

$$A^{-1} = \frac{1}{(\mu+\gamma+m_{21})(\mu+\gamma+m_{12}) - m_{21}m_{12})} \begin{pmatrix} \mu+\gamma+m_{12} & m_{12} \\ m_{21} & \mu+\gamma+m_{21} \end{pmatrix},$$

$$B^{-1} = \frac{1}{(\mu+k+m_{21})(\mu+k+m_{12}) - m_{21}m_{12}} \begin{pmatrix} \mu+k+m_{12} & m_{12} \\ m_{21} & \mu+k+m_{21} \end{pmatrix}.$$

To simplify calculations we introduce the substitutions

$$\begin{aligned} d_1 &= \mu+\gamma+m_{21} \\ d_2 &= \mu+\gamma+m_{12} \\ e_1 &= \mu+k+m_{21} \\ e_2 &= \mu+k+m_{12} \end{aligned}$$

Thus providing a simplified form of the matrices A^{-1} and B^{-1}:

$$A^{-1} = \frac{1}{d_1d_2 - m_{21}m_{12}} \begin{pmatrix} d_2 & m_{12} \\ m_{21} & d_1 \end{pmatrix},$$

$$B^{-1} = \frac{1}{e_1e_2 - m_{21}m_{12}} \begin{pmatrix} e_2 & m_{12} \\ m_{21} & e_1 \end{pmatrix}.$$

Substituting into the general form of R_0 and finding the dominant eigenvalue yields:

$$\begin{aligned} R_0 &= \rho\left(\frac{1}{(e_1e_2 - m_{21}m_{12})(d_1d_2 - m_{21}m_{12})} \begin{pmatrix} \beta e_2 & \beta m_{12} \\ \beta m_{21} & \beta e_1 \end{pmatrix} \begin{pmatrix} kd_2 & km_{12} \\ km_{21} & kd_1 \end{pmatrix}\right) \\ &= \frac{1}{2}k\beta\left(\frac{d_1e_1 + d_2e_2 + 2m_{12}m_{21} + \sqrt{(d_1e_1 - d_2e_2)^2 + 4m_{12}m_{21}(d_1+e_1)(d_2+e_2)}}{(d_1d_2 - m_{12}m_{21})(e_1e_2 - m_{12}m_{21})}\right) \end{aligned}$$

Even though this is a complicated expression to analyze, a bounding interval for R_0 can be found.

$$
\begin{aligned}
R_0 &> \frac{1}{2}k\beta\left(\frac{d_1e_1+d_2e_2+2m_{12}m_{21}+\sqrt{(d_1e_1-d_2e_2)^2}}{(d_1d_2-m_{12}m_{21})(e_1e_2-m_{12}m_{21})}\right)\\
&= \frac{1}{2}k\beta\left(\frac{d_1e_1+d_2e_2+2m_{12}m_{21}+|d_1e_1-d_2e_2|}{(d_1d_2-m_{12}m_{21})(e_1e_2-m_{12}m_{21})}\right)\\
&= \frac{1}{2}k\beta\left(\frac{2\max(d_1e_1,d_2e_2)+2m_{12}m_{21}}{(d_1d_2-m_{12}m_{21})(e_1e_2-m_{12}m_{21})}\right)\\
&= k\beta\frac{\max(d_1e_1,d_2e_2)+m_{12}m_{21}}{(d_1d_2-m_{12}m_{21})(e_1e_2-m_{12}m_{21})}
\end{aligned}
$$

Thus,

$$
R_0 > k\beta\frac{\max(d_1e_1,d_2e_2)+m_{12}m_{21}}{(d_1d_2-m_{12}m_{21})(e_1e_2-m_{12}m_{21})}
$$

Additionally,

$$
\begin{aligned}
R_0 &< \frac{1}{2}k\beta\left(\frac{d_1e_1+d_2e_2+2m_{12}m_{21}+\sqrt{(d_1e_1-d_2e_2)^2}+\sqrt{4m_{12}m_{21}(d_1+e_1)(d_2+e_2)}}{(d_1d_2-m_{12}m_{21})(e_1e_2-m_{12}m_{21})}\right)\\
&= k\beta\left(\frac{\max(d_1e_1,d_2e_2)+m_{12}m_{21}+\sqrt{m_{12}m_{21}(d_1+e_1)(d_2+e_2)}}{(d_1d_2-m_{12}m_{21})(e_1e_2-m_{12}m_{21})}\right)
\end{aligned}
$$

Thus,

$$
R_0 < k\beta\left(\frac{\max(d_1e_1,d_2e_2)+m_{12}m_{21}+\sqrt{m_{12}m_{21}(d_1+e_1)(d_2+e_2)}}{(d_1d_2-m_{12}m_{21})(e_1e_2-m_{12}m_{21})}\right)
$$

Therefore, for a two city system

$$
k\beta\frac{\max(d_1e_1,d_2e_2)+m_{12}m_{21}}{(d_1d_2-m_{12}m_{21})(e_1e_2-m_{12}m_{21})} < R_0 < k\beta\left(\frac{\max(d_1e_1,d_2e_2)+m_{12}m_{21}+\sqrt{m_{12}m_{21}(d_1+e_1)(d_2+e_2)}}{(d_1d_2-m_{12}m_{21})(e_1e_2-m_{12}m_{21})}\right)
$$

R_0 for a Partitioned Model with n Cities

To apply the results of Arino et al. define the X vector as

$$
X = (L_{T1}, L_{R1}, L_{T2}, L_{R2}, \ldots, L_{Tn}, L_{Rn}, I_{T1}, I_{R1}, I_{T2}, I_{R2}, \ldots, I_{Tn}, I_{Rn})^T
$$

Again the f vector contains all the terms of the latent and infected that result in new infections while the v vector contains the negative of the remaining terms.

$$f = \begin{pmatrix} \frac{\beta S_{T1}(I_{T1}+I_{R1})}{N_1} \\ \frac{\beta S_{R1}(I_{T1}+I_{R1})}{N_1} \\ \vdots \\ \frac{\beta S_{Tn}(I_{Tn}+I_{Rn})}{N_n} \\ \frac{\beta S_{Rn}(I_{Tn}+I_{Rn})}{N_n} \\ 0 \\ \vdots \\ \vdots \\ 0 \end{pmatrix}, v = \begin{pmatrix} (\mu+k)L_{T1} - \sum_{j=1}^{n} m_{1j}L_{Tj} + \sum_{j=1}^{n} m_{j1}L_{T1} \\ (\mu+k)L_{R1} \\ \vdots \\ (\mu+k)L_{Tn} - \sum_{j=1}^{n} m_{nj}L_{Tj} + \sum_{j=1}^{n} m_{jn}L_{Tn} \\ (\mu+k)L_{Rn} \\ (\mu+\gamma)I_{T1} - kL_{T1} - \sum_{j=1}^{n} m_{1j}I_{T1} + \sum_{j=1}^{n} m_{j1}I_{T1} \\ (\mu+\gamma)I_{R1} - kL_{R1} \\ \vdots \\ (\mu+\gamma)I_{Tn} - kL_{Tn} - \sum_{j=1}^{n} m_{nj}I_{T1} + \sum_{j=1}^{n} m_{jn}I_{T1} \\ (\mu+\gamma)I_{Rn} - kL_{Rn} \end{pmatrix}$$

For the G matrix a substitution is used to simplify the problem. At the DFE each susceptible class has the same population as its initial conditions that is $S_{Ti} = N_{Ti}$ and $S_{Ri} = N_{Ri}$ also Let $P_l = \frac{N_{Tl}}{N_l}$, where N_{Tl} is the transitive population of city l and N_l is the total population of city l. Then, 1-P_l = 1-$\frac{N_{Tl}}{N_l} = \frac{N_l - N_{Tl}}{N_l} = \frac{N_{Rl}}{N_l}$. We then redefine our G Matrix as

$$G = \beta \begin{pmatrix} \begin{pmatrix} P_1 & P_1 \\ 1-P_1 & 1-P_1 \end{pmatrix} & \begin{pmatrix} 0 & 0 \\ 0 & 0 \end{pmatrix} & \cdots & \begin{pmatrix} 0 & 0 \\ 0 & 0 \end{pmatrix} \\ \begin{pmatrix} 0 & 0 \\ 0 & 0 \end{pmatrix} & \begin{pmatrix} P_2 & P_2 \\ 1-P_2 & 1-P_2 \end{pmatrix} & & \begin{pmatrix} 0 & 0 \\ 0 & 0 \end{pmatrix} \\ \vdots & & \ddots & \vdots \\ \begin{pmatrix} 0 & 0 \\ 0 & 0 \end{pmatrix} & \begin{pmatrix} 0 & 0 \\ 0 & 0 \end{pmatrix} & \cdots & \begin{pmatrix} P_n & P_n \\ 1-P_n & 1-P_n \end{pmatrix} \end{pmatrix},$$

The B, C, and A matrices are defined as below

$$A = \begin{pmatrix} \begin{pmatrix} \mu+k+\sum_{j=1}^{n} m_{ji} & 0 \\ 0 & \mu+k \end{pmatrix} & \begin{pmatrix} -m_{21} & 0 \\ 0 & 0 \end{pmatrix} & & \begin{pmatrix} -m_{1n} & 0 \\ 0 & 0 \end{pmatrix} \\ \begin{pmatrix} -m_{21} & 0 \\ 0 & 0 \end{pmatrix} & \begin{pmatrix} \mu+k+\sum_{j=1}^{n} m_{j2} & 0 \\ 0 & \mu+k \end{pmatrix} & \cdots & \begin{pmatrix} -m_{2n} & 0 \\ 0 & 0 \end{pmatrix} \\ & & \ddots & \vdots \\ \begin{pmatrix} -m_{n1} & 0 \\ 0 & 0 \end{pmatrix} & \begin{pmatrix} -m_{n2} & 0 \\ 0 & 0 \end{pmatrix} & \cdots & \begin{pmatrix} \mu+k+\sum_{j=1}^{n} m_{jn} & 0 \\ 0 & 0 \end{pmatrix} \end{pmatrix},$$

$$B = \begin{pmatrix} \begin{pmatrix} \mu+\gamma+\sum_{j=1}^{n} m_{ji} & 0 \\ 0 & \mu+\gamma \end{pmatrix} & \begin{pmatrix} -m_{21} & 0 \\ 0 & 0 \end{pmatrix} & \cdots & \begin{pmatrix} -m_{1n} & 0 \\ 0 & 0 \end{pmatrix} \\ \begin{pmatrix} -m_{21} & 0 \\ 0 & 0 \end{pmatrix} & \begin{pmatrix} \mu+\gamma+\sum_{j=1}^{n} m_{j2} & 0 \\ 0 & \mu+\gamma \end{pmatrix} & \cdots & \begin{pmatrix} -m_{2n} & 0 \\ 0 & 0 \end{pmatrix} \\ \vdots & & \ddots & \vdots \\ \begin{pmatrix} -m_{n1} & 0 \\ 0 & 0 \end{pmatrix} & \begin{pmatrix} -m_{n2} & 0 \\ 0 & 0 \end{pmatrix} & \cdots & \begin{pmatrix} \mu+\gamma+\sum_{j=1}^{n} m_{jn} & 0 \\ 0 & 0 \end{pmatrix} \end{pmatrix},$$

$C = diag(k)$.

Again $R_0 = \rho(GB^{-1}CA^{-1})$ with the A,B,C,G matrices for this system. Note that the elements of these matrices are not matrices as well. This notation is only used to represent they patterned behavior of their elements

7 Numerical Results

The partitioned and non-partitioned models act quite similarly in overall behavior, but many cities show a time lag in their behavior between the two models (See Figure 3 for example). More specifically, disease spread occurs faster in the non-partitioned model than in the partitioned model–the initial city loses infected individuals faster, and the other cities gain them sooner.

All numerical solutions to the systems were run using baseline SARS data ($\beta = .25, k = \frac{1}{6.37}, \gamma = \frac{1}{28.4}$) from Chowell and Castillo-Chavez [6]. We look at a system consisting of the 34 largest cities in the United States, for which airline/population data was gathered from the United States 2000 census by Hyman and LaForce [12]. This data assumes balanced migrations between cities; that is, $\alpha_{ij} = \alpha_{ji}$. Due to the assumption of balanced migration, the sums of the inward and outward migrations across all classes in a city are equal; therefore, the population is constant within a city and over the entire system. In this data, α_{ii} is considered to be zero $\forall i$, and because not all α_{ij} terms are nonzero, the network is not fully connected. See Figure ?? for city populations and Figure ?? for flight data. Traveler populations were assumed to be 10 percent of the entire population of their respective cities, the initial number of infected individuals was held at .0001 percent of the entire system population (approximately 107 individuals), and natural birth/death rates were assumed to be very low (around .0002740, a number gathered from [12]). These parameters give us an R_0 greater than one for each run.

7.1 Partitioned Model Results

In order to study how migration affects disease spread in the 34-city network, we found numerical solutions to our system using Matlab's built-in one-step ODE45 solver, which is an implementation of the Dormand-Prince pair explicit Runge-Kutta (4,5) formula. For each of the 34 cities, we look at disease spread at several different time steps (Figure 4) and at day 35 (35 days is the average time from initial infection with SARS to recovery) as shown in Figure 5.

Here we consider disease spread to be the proportion of infected individuals in the total secondary population ($\sum_{j\neq i}^{n} \frac{I_{Tj}+I_{Rj}}{N_j}$ where the ith city is the initial host) at a given time. Disease parameters and initial number of infected individuals was held constant for each run. At any

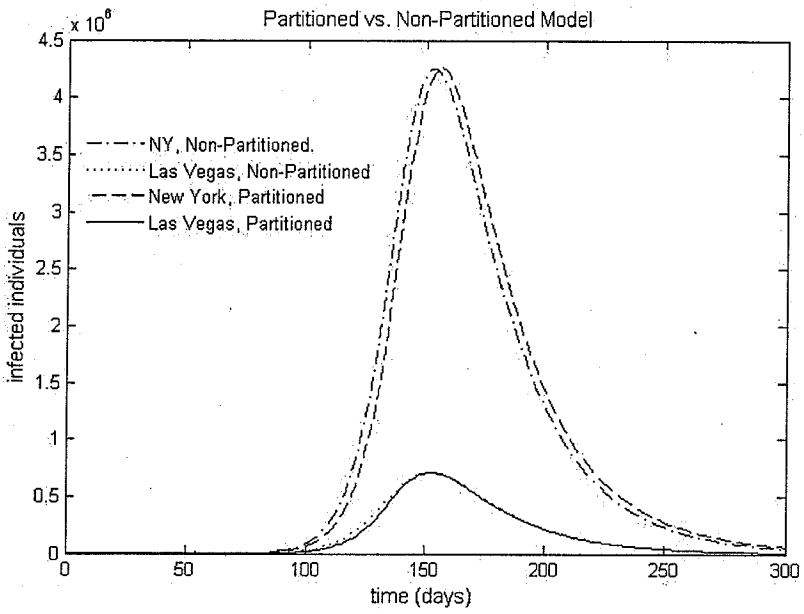

Figure 3: Behavior of Partitioned and Non-Partitioned Models

time step, looking at this information against the proportional outward migration rate for city i ($\sum_{j=1}^{n} \frac{\alpha_{ji}}{N_i}$) yields a scatter plot that looks very logarithmic (Figure 4), and indeed when this is plotted on a log scale for day 35, the data shows a highly significant (p = .000 within Minitab's tolerance) linear trend (See Figure 5). A linear fit is appropriate for the log-transformed data, with $R^2 = 98.5\%$. Since each initial host city represents a point on this graph, we can sort the list of cities in order of descending importance in Figure 5, and this tells which cities spread disease to the rest of the network the fastest or slowest (see Table 2).

Fastest Spreaders	Slowest Spreaders
Las Vegas	Philadelphia
Orlando	Pittsburgh
San Francisco	Cleveland
Denver	Cincinatti
Ft. Lauderdale	San Antonio
Dallas	Milwaukee
Seattle	Miami

Table 2: Fastest and Slowest Spreaders–Partitioned Model

We also looked at a theoretical homogeneous system ($N_i = N \; \forall \; i$ and $\alpha_{ji} = \alpha \; \forall \; (i,j)$ such that $i \neq j$, where N and α are constants). We varied migration rates by scaling the matrix $\{\alpha\}$ by different scalars and observing system response. As can be seen in Figure 6, the theoretical system

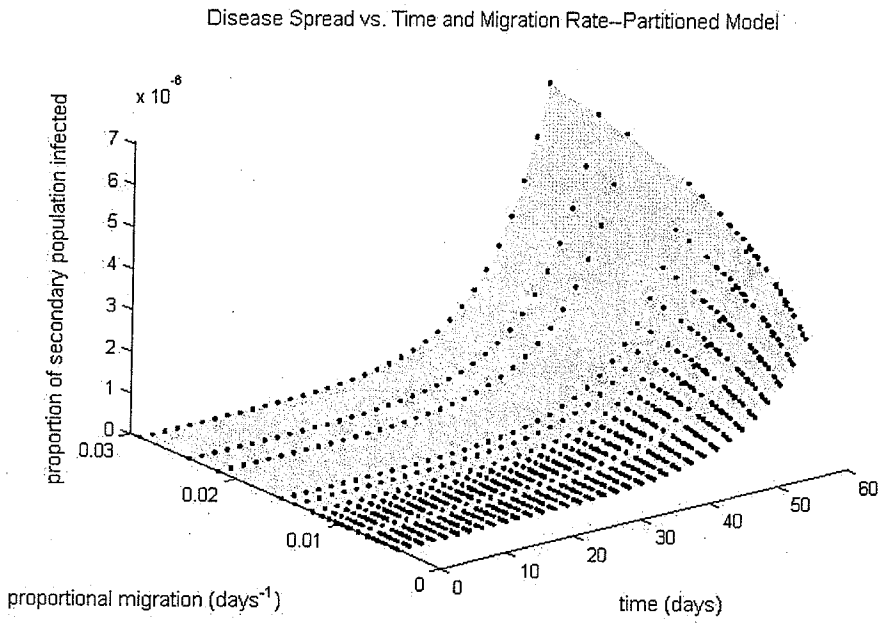

Figure 4: The Effect of Proportional Outward Migration Rate ($\sum_{j=1}^{n} \frac{\alpha_{ji}}{N_i}$) on Initial Disease Spread over Multiple Time Steps in the Partitioned Model

responded to changes in migration rate in a logarithmic manner, much as the real-world 34-city system is sensitive to the migration rate of the initial host city. We have no explanation as yet for the small dip in the curve around proportional migration = .01, but would like to study it further if we can determine that it is not due to numerical error.

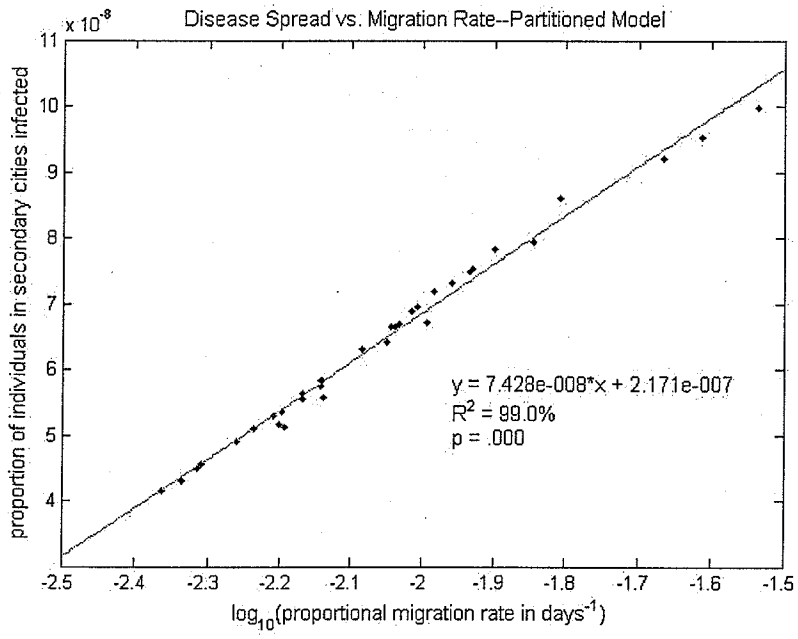

Figure 5: The Effect of Proportional Outward Migration Rate ($\sum_{j=1}^{n} \frac{\alpha_{ji}}{N_i}$) on Initial Disease Spread in the Partitioned Model

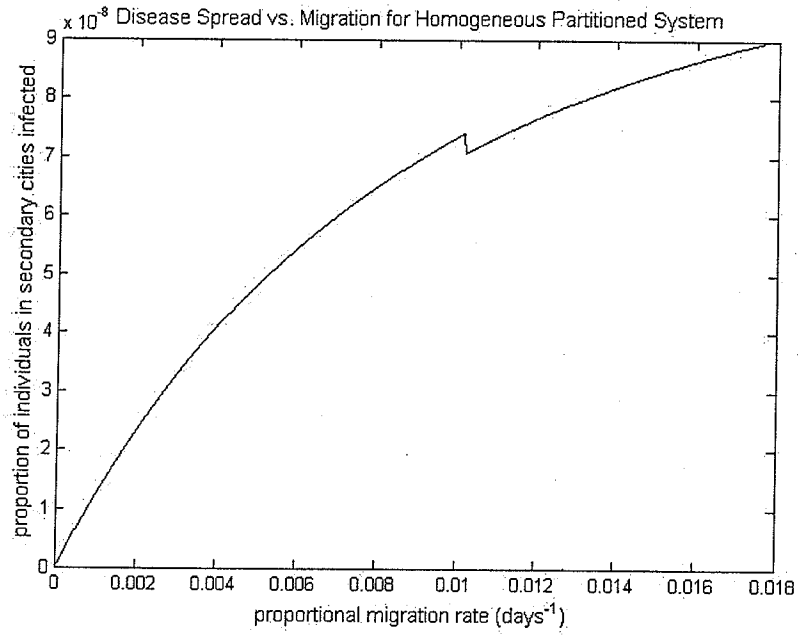

Figure 6: The Effect of Migration Rate in a Homogenous System in the Partitioned Model

We were also interested at looking at the effect of connectivity upon initial disease spread. Here we consider connectivity of city i to be the number of cities to which it is adjacent by air traffic (that is, the number of integer values $j \in [1, 34]$ for which $\alpha_{ji} > 0$). We expected there to be a loose correlation between connectivity and disease spread from city i (defined as above). Upon creating a scatter plot of the disease spread from city i at day 35 versus its connectivity (see Figure 7), we see a vague positive trend; however, an ANOVA test shows that this trend is not statistically significant (p = .065).

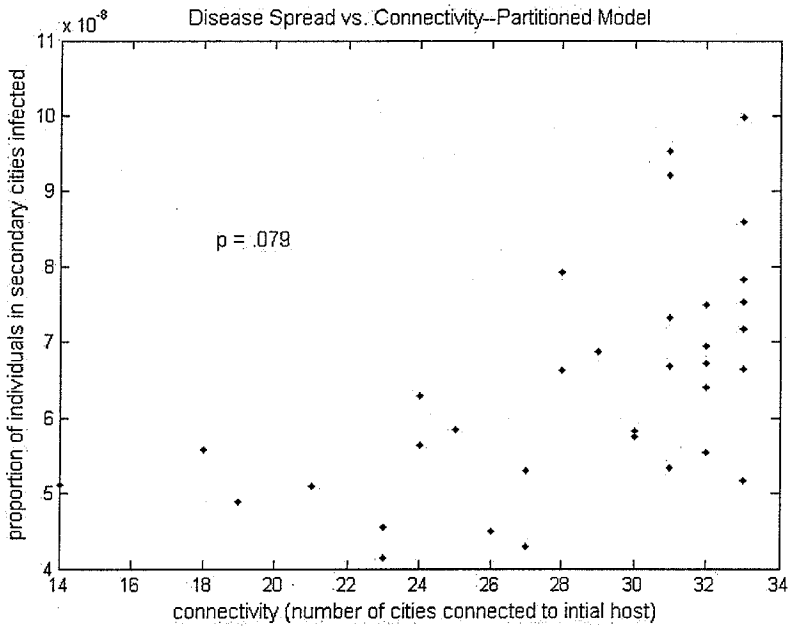

Figure 7: The Effect of Connectivity on Initial Disease Spread in the Partitioned Model

7.2 Non-Partitioned Model Results

While the non-partitioned model acts fairly similarly to the compartmental model, there are several interesting differences to be highlighted. Using the same methods as those for the compartmental model, we look at disease spread vs. migration throughout time (Figure 8), disease spread vs. migration at day 35 for both the real network (Figure 9) and the homogenous network (Figure 10), which cities spread disease the fastest and slowest (Table 3), and disease spread vs. connectivity (Figure 11). Of interest is how neither the real nor the homogeneous systems respond exactly the same way to the non-partitioned model as they do to the partitioned; namely, the growth of disease spread does not slow down as quickly, and almost fits a linear curve rather than a log-linear curve. Also of interest is that some of the cities in the fastest/slowest spreaders list are slightly interchanged, and that the tenuous correlation between disease spread and connectivity is even less significant (an ANOVA test yields p = .325) in the non-partitioned model.

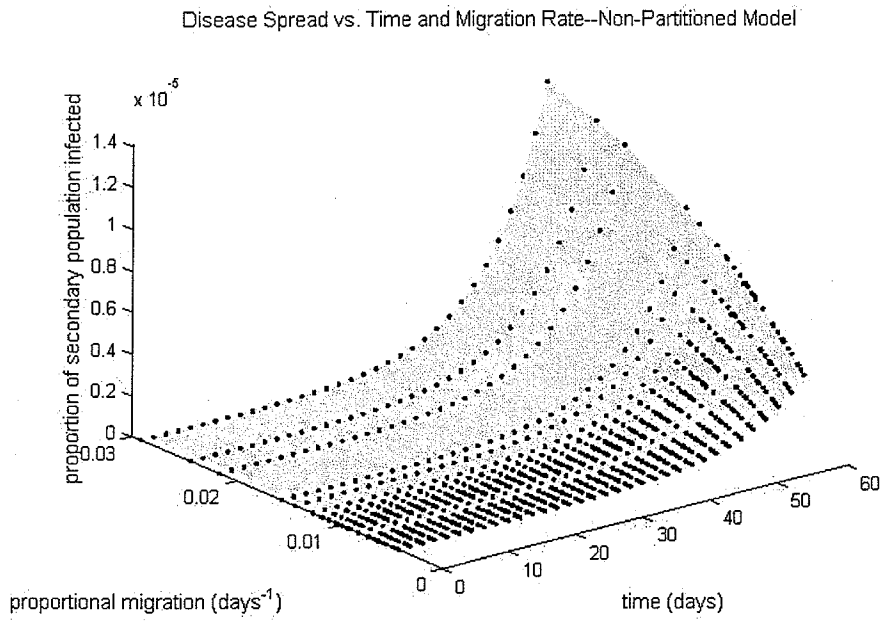

Figure 8: The Effect of Outward Proportional Migration Rate ($\sum_{j=1}^{n} \frac{\alpha_{ji}}{N_i}$) on Initial Disease Spread Over Multiple Time Steps in the Non-Partitioned Model

Fastest Spreaders	Slowest Spreaders
Las Vegas	Pittsburgh
San Francisco	Philadelphia
Orlando	Cleveland
Denver	Cincinatti
Ft. Lauderdale	San Antonio
Seattle	Milwaukee
Dallas	Miami

Table 3: Fastest and Slowest Spreaders in the Non-Partitioned Model

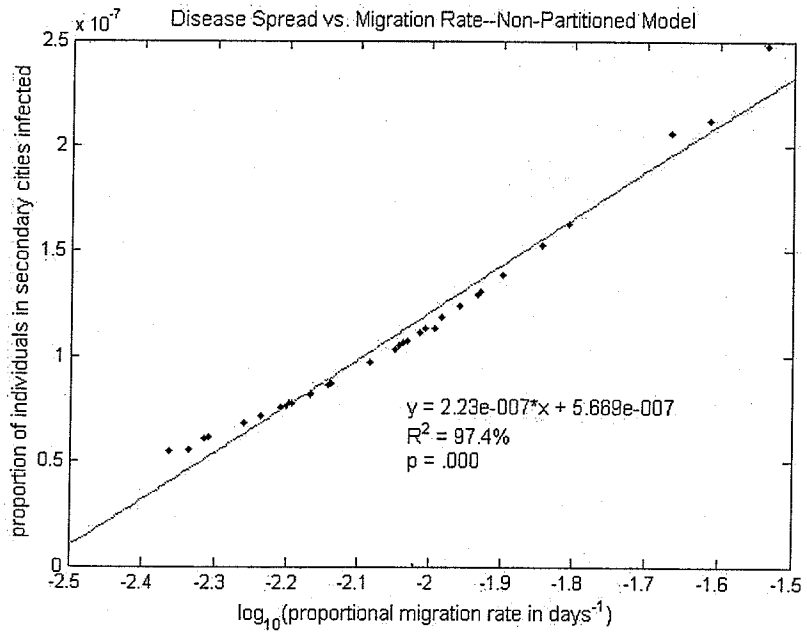

Figure 9: The Effect of Outward Proportional Migration Rate ($\sum_{j=1}^{n} \frac{\alpha_{ji}}{N_i}$) on Initial Disease Spread in the Non-Partitioned Model

As in the partitioned model, the homogeneous system responds similarly to the real-world system in regards to proportional migration rates (Figure 10). (Note that while in the real-world system we are looking only at the migration rate of the initial host city, in the homogeneous network we are looking at migration rate of the initial host city *and* that of the rest of the system. Increasing the migration rates for the entire system may increase disease spread faster than just the rate for the initial host city, since secondary cities can also spread the disease to one another faster). Note how secondary infections increase almost linearly (rather than logarithmically) with respect to increasing migration rate, showing that the effects of migration saturate more quickly in the partitioned system than in the non-partitioned.

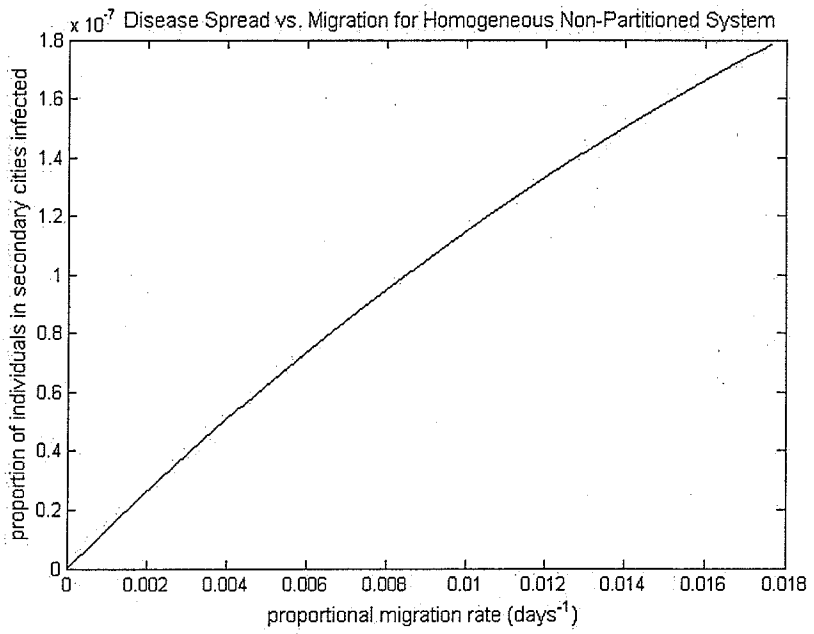

Figure 10: The Effect of Migration Rate in a Homogenous System in the Non-Partitioned Model

Much like the partitioned model, there is a tenuous trend in the non-partitioned model for disease spread to increase with number of connections (Figure 11); however, this trend is statistically insignificant ($p = .325$). While the biggest spreaders have high connectivity, the reverse is not always true.

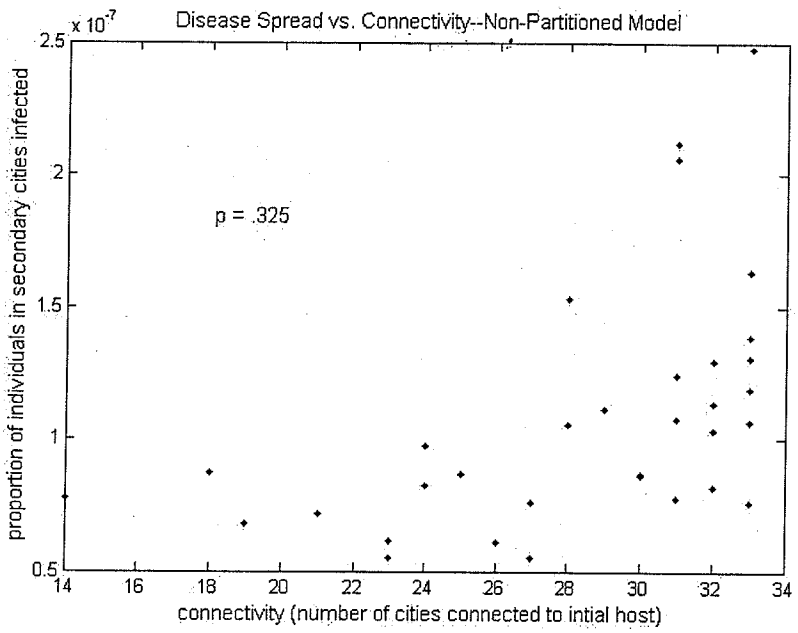

Figure 11: The Effect of Connectivity on Initial Disease Spread in the Non-Partitioned Model

7.3 R_0

Numerically computing R_0 for different scalar multiples of the migration matrix shows that R_0 is virtually insensitive to changes in migration. While we know analytically that R_0 depends on migration, we also know that because of the structure of R_0 (see the two-city R_0 for example) and because m_{ij} terms are relatively small (orders of magnitude smaller than all other parameters), other terms in the calculation of R_0 should dominate. This is exemplified in our numerical work. We consider thousands of scalar values uniformly distributed between 0 and 2, and for each scalar value c we calculate R_0 with a new migration matrix that is given by cM_1, where M_1 is the original migration matrix. All R_0 values found were identical to the thirteenth decimal place. The difference between any two adjacent R_0 values (that is, $[R_0(c_{i+1}) - R_0(c_i)]$ for any i) has an absolute value bounded by 8×10^{-14}, and appears to be random with normal distribution around mean 0. This seems to suggest that numerical error of the algorithm is more responsible for numerical changes in R_0 than migration is, and thus that migration is effectively insignificant in the calculation of R_0 for the system defined by our data.

8 Discussion

While the partitioned and non-partitioned models have some slight differences (for instance, many cities experience a time lag between their behavior in the two models, and when looking at disease spread, some cities become more important in one model than in the other) the general behavior of the epidemic over both models is very similar. This suggests that although the partitioned model may be more realistic, simplifying to the more general non-partitioned model does not cause any drastic losses of information or accuracy.

The results of looking at disease spread vs. migration rate in both the partitioned and non-partitioned models strongly suggest that the proportional outward migration rate of the initial host city is the determining factor in the speed of disease spread, at least in the initial period before the epidemic hits is peak. This seems fairly intuitive, as secondary cities can only be infected by the initial host city, and the rate of migration of infected individuals from the host city is determined by $\sum_{j=1}^{n} \alpha_{ji}\frac{I_i}{N_i}$. Of interest, however, is the difference in the behavior of the two models regarding this outward migration rate: while the effect of migration rate quickly saturates in the partitioned model, it saturates much more slowly in the non-partitioned model. This is probably due to the fact that since N_{Ti} is significantly smaller than N_i, $\frac{I_{Ti}}{N_{Ti}}$ in the partitioned model can increase more quickly than $\frac{I_i}{N_i}$ in the non-partitioned model, so the effect of migration rate is overshadowed more quickly by the infection term.

The result that connectivity of the initial host city does not have any obvious correlation with disease spread is quite interesting. This result most likely stems from the fact that although highly-connected cities are more likely to have large migration rates than are cities with lower connectivity numbers, it is not a perfect correlation, and such highly-connected cities are most likely large, so $\sum_{j=1}^{n} \alpha_{ji}\frac{I_i}{N_i}$ may actually be lower than that of a city with fewer connections. Since it is clear that proportional outward migration of the initial host city is the main determinant of secondary disease magnitude in early initial periods, it is intuitive that if there is only a weak correlation between connectivity and migration, then there would only be a weak correlation between connectivity and initial disease spread.

Our finding that R_0 is numerically insensitive to migration is intuitive, since disease dynamics should be the determining factor in reproductive ratio. This finding does not imply, however, that migration is unimportant; while it does not affect reproductive ratio, it can determine which cities

are most at risk and when, and which cities can spread the disease the fastest. When one takes into account the fact that behavioral effects and quarantine can play a significant role in later behavior, such initial differences can become quite important to overall behavior of the disease.

9 Future Work

Further study is required to better understand the effect of connectivity as well as migration on the system. For the models presented here sensitivity analysis on R_0 , $\frac{dI}{dt}$, and other quantities with respect to the migration parameters would more fully explain how changes on migration would effect the diseases ability to propagate through the system. Also the issue of how the number of connections would distribute the disease would be best studied by generating random graphs with n connections between a set number of cities. For each value of n a large sampling of random graphs would be required to generate an average behavior. Since behavioral change after the discovery of the disease would most likely decrease migration rates (and probably β as well), an adaptation of these models could be considered where the migrations (and other parameters) would be a decreasing function of time. Here it was also assumed that each class had an equal opportunity to migrate to another city. This is an unrealistic assumption that was made for simplicity. It would be more likely for a more violent disease that the infectious class would travel less and that the disease would be spread by the latent persons who become infectious at their new destination.

Due to the large difference in size between the populations of the cities and the number of people who travel in one day, and due to the fact that numbers of infected individuals will most likely be low at the beginning of an epidemic, stochastic or agent based models may be a more accurate method of modeling these kind of systems. Some method of randomly sampling the city population for migration could cause variations in the number of infected persons who move from one city to another. If the infectious persons travel at a slower rate then random sampling and stochastic models may result in an entire migratory group being disease free in one or more time intervals. In a deterministic model a large quantity of infected persons must be introduced in order to accurately while in the case of SARS moving from Hong Kong to Toronto only a single individual was involved. This further suggests that stochastic and agent based models would result in behaviors in the disease that would not be seen in a deterministic model.

Lastly the disease parameters and characteristics can change the entire multi-city system. If the disease requires close continuous contact with a person, then a transitive population would not be the deciding factor on how the disease spreads, but rather the number of contacts per individual at each city. Similarly the rate of infection may not be linearly proportional to population, in which case it would be different in each city–for instance, cities with higher population densities would probably have a higher contact rate. If the disease had a short time of incubation and a high mortality rate, then behavioral effects would more quickly change the migrations. All these possible effects could be taken into consideration, if not with a deterministic model, perhaps with stochastic or agent-based methods.

10 Acknowledgements

We would like to express our appreciation to the many people who offered their time and effort in contributing to this project: Armando Arciniega, Leon Arriola, Fred Brauer, Carlos Castillo-Chavez, Gerardo Chowell, James Hyman, Richard Jordan, Christopher Kribs-Zaleta, Benjamin Morin, Stephen Tennenbaum, and the entire MTBI/LANL community.